Analytical Biochemistry 529 (2017) 117–126

Contents lists available at ScienceDirect

Analytical Biochemistry

journal homepage: www.elsevier.com/locate/yabio

Technical and experimental features of Magnetic Resonance Spectroscopy of brain glycogen metabolism

Ana Francisca Soares [a], Rolf Gruetter [a, b, c, d], Hongxia Lei [b, c, *]

[a] Laboratory for Functional and Metabolic Imaging (LIFMET), École Polytechnique Fédérale de Lausanne (EPFL), Lausanne, Switzerland
[b] Department of Radiology, University of Genève (UNIGE), Switzerland
[c] Center for Biomedical Imaging (CIBM), Lausanne, Switzerland
[d] Department of Radiology, University of Lausanne (UNIL), Switzerland

ARTICLE INFO

Article history:
Received 20 April 2016
Received in revised form
31 August 2016
Accepted 23 December 2016
Available online 26 December 2016

ABSTRACT

In the brain, glycogen is a source of glucose not only in emergency situations but also during normal brain activity. Altered brain glycogen metabolism is associated with energetic dysregulation in pathological conditions, such as diabetes or epilepsy. Both in humans and animals, brain glycogen levels have been assessed non-invasively by Carbon-13 Magnetic Resonance Spectroscopy (^{13}C-MRS) *in vivo*. With this approach, glycogen synthesis and degradation may be followed in real time, thereby providing valuable insights into brain glycogen dynamics. However, compared to the liver and muscle, where glycogen is abundant, the sensitivity for detection of brain glycogen by ^{13}C-MRS is inherently low. In this review we focus on strategies used to optimize the sensitivity for ^{13}C-MRS detection of glycogen. Namely, we explore several technical perspectives, such as magnetic field strength, field homogeneity, coil design, decoupling, and localization methods. Furthermore, we also address basic principles underlying the use of ^{13}C-labeled precursors to enhance the detectable glycogen signal, emphasizing specific experimental aspects relevant for obtaining kinetic information on brain glycogen.

1. Introduction

Glucose is a universal energy fuel whose oxidation supports cellular work. The brain, in particular, is highly dependent on glucose oxidation and is, therefore, responsible for a substantial fraction of basal blood glucose uptake [1]. Mammalian cells obtain glucose not only from the blood but also from intracellular stores located in the cytosol. In these stores glucose exists as a polymer: glycogen. Polymerization allows for the presence of large amounts of glucose inside the cell without consequences to osmolality or concentration-gradient based exchanges with the blood, where physiological glucose concentration is ~5 mM. Glycogen is found in several organs, including the brain. In this review we briefly overview the biochemistry, structure and function of glycogen, as elucidated mainly by studies performed in the liver and skeletal muscle, the two largest stores of glycogen in the body. Then, we focus on the role of glycogen in the brain and give some examples of altered glycogen metabolism in human diseases.

Magnetic resonance (MR) methods *in vivo*, notably MR spectroscopy (MRS), are a unique and versatile tool to assess metabolite concentrations in a given organ, and to follow their dynamic changes non-invasively and in real time. Carbon-13 MRS (^{13}C-MRS) is currently the state-of-the-art technique to study glycogen metabolism *in vivo* in humans and rodents. Such studies have explored glycogen dynamics under different physiological conditions and have been expertly discussed in a recent review by Khowaja et al. [2]. Therefore, in the second half of this review, we rather focus on relevant technical and experimental aspects that should be considered for optimization of glycogen detection and data interpretation.

List of abbreviations: ^{1}H-MRS, Proton magnetic resonance spectroscopy; ^{13}C-MRS, Carbon-13 magnetic resonance spectroscopy; B_0, magnetic field; CEST, Chemical exchange saturation transfer; CSI, Chemical shift imaging; FID, Free induction decay; FSW, Fourier series window; FWHM, Full width at half maximum; ISIS, Image selective *in vivo* spectroscopy; MR, magnetic resonance; MRI, magnetic resonance imaging; MRS, magnetic resonance spectroscopy; NOE, Nuclear Overhauser effect; OVS, Outer volume suppression; RF, Radio-frequency; SAR, Specific absorption rates; SNR, Signal to noise ratio; T_1, Spin-lattice relaxation time; T_2, Spin-spin relaxation time; UDP, Uridine diphosphate; VOI, Volume of interest; γ, Gyromagnetic ratio; $\gamma\Delta B_0$, Field inhomogeneity.

* Corresponding author. EPFL-SB-CIBM-AIT, CH F1 627 Ecole Polytechnique Fédérale de Lausanne, 1015 Lausanne, Switzerland.
E-mail address: hongxia.lei@epfl.ch (H. Lei).

http://dx.doi.org/10.1016/j.ab.2016.12.023
0003-2697/

2. Glycogen biochemistry structure and function

Mammalian glycogen is composed of several chains of 11–16 glucose molecules [3] linked by linear α-(1,4) glucosidic bonds or branching α-(1,6) glucosidic bonds [4]. The succession of branches forms a bush-shaped spherical particle (β-particle) organized in tiers, with an average diameter of ~20 nm [5]. This structure is optimized to be stored in the smallest possible volume while keeping the glucosyl units easily accessible to enzymes involved in glycogen metabolism [6]. The glycogen molecule is built from a protein primer, glycogenin [7], and it is now clear that glycogen is directly associated to several other proteins, including those involved in its own metabolism (*e.g.* glycogen synthase, glycogen phosphorylase, or glycogen branching and debranching enzymes) and other metabolically relevant ones [8]. Because these glycogen granules are actually a collective structure of polysaccharide chains with their own metabolic machinery they have been referred to as an organelle-type particle, the so-called glycosome [9].

Glycogen granules assume different structural organizations depending on the tissue of origin and in accordance with the function they serve. For instance, in skeletal muscle, glycogen exists mostly as ~20 nm β-particles, also called proglycogen, whose size may reach up to ~40 nm (macroglycogen) with the addition of more glucosyl units [8]. The abundance of smaller proglycogen particles, with a proportionally higher content of metabolically active enzymes, seems to serve the purpose of ensuring a readily expendable glucose source for muscular work [8]. On the other hand, in the liver and cardiac muscle, β-particles are often clustered into larger aggregates of ~150 nm: α-particles [10]. Such aggregation occurs presumably via covalent or strong non-covalent bonds [11]. Differently from skeletal muscle glycogen, these larger particles with a proportionally lower protein content [9] would be in line with a slower mobilization of glucosyl units for hepatic glucose output during progressive fasting. Interestingly, the formation of α-particles in the liver appears to occur during net glycogen degradation, providing a mechanism to control glucose release [12,13].

3. Brain glycogen

Brain metabolism mainly relies on glucose oxidation. Glycogen represents the largest store of glucose equivalents in the brain [14] with its concentrations ranging from 3 μmol/g[1] to 10 μmol/g in the rodent [15–20] and human brain [21]. Glycogen concentration exhibits regional differences [16,17,22–25], *e.g.* reaching over 20 μmol/g in corpus callosum of rats [17].

Structurally, glycogen exists both as β- and α-particles in astrocytes [26]. Despite expressing all the necessary enzymes for glycogen synthesis, this pathway remains mostly inactive in neurons [27]. At the cellular level, glycogen biogenesis from glucose requires the sequential activities of hexokinase (glucose → glucose-6-phosphate), phosphoglucomutase (glucose-6-phosphate → glucose-1-phosphate), uridine diphosphate (UDP)-glucose pyrophosphorylase (glucose-1-phosphate → UDP-glucose) and glycogen synthase, which adds glucosyl residues from UDP-glucose to the glycogen molecule via α-(1,4) bonds. Branching of the glycogen molecule is afforded by the branching enzyme that catalyzes the formation of α-(1,6) glucosidic bonds. By glycogen phosphorylase activity, glucosyl units are released from glycogen in the form of glucose-1-phosphate, and this intermediate is further converted to glucose-6-phosphate by phosphoglucomutase activity.

While it is generally accepted that brain glycogen is not a first-line oxidative fuel, it becomes metabolically relevant under conditions where energy demand can no longer be met by blood-derived glucose. Indeed, a large body of pre-clinical studies demonstrates such glycogen-dependent neuronal activity in stress situations. Illustrative examples comprise the reduction of brain glycogen levels during intense exercise [28], hypoglycemia [29,30], global ischemia [22] or sleep deprivation [17]. Importantly, it is now recognized that glycogen is key for normal brain function beyond representing an emergency energy reserve [16]. For example, glycogen has been proposed as an expeditious energy source supporting glutamatergic neurotransmission [31]. In agreement, brain glycogen was shown to be of particular relevance during brain activation [32,33] and learning [34–36], when increasing energy demands need to be rapidly met. Conversely, cerebral glycogen stores have to be adequately replenished when neuronal activity is low and a glucose surplus is available, what has been shown to occur during anesthesia, sleeping or hibernation [16].

Therefore, glycogen metabolism in the brain is a highly dynamic process that adapts to activation and resting periods in a complementary fashion. For instance, brain glycogen levels may double relative to the basal when recovering from severe hypoglycemia [29,37], intensive exercise [28], and sleep deprivation [17,38]. This phenomenon closely resembles glycogen supercompensation as described in the skeletal muscle after exercise [39], suggesting a similar organization of glycogen and associated enzymatic machinery in both tissues. Indeed, the muscle isoforms of glycogen synthase and phosphorylase (which are mostly found but not restricted to the skeletal muscle) are also expressed in the brain [40].

The metabolic pathways downstream glycogen degradation that are involved in supporting brain energy metabolism remain to be fully characterized. Although efforts have been made to understand the precise fate of mobilized glycogen carbons, this topic is still subject of debate. Glycogen-derived glucose-6-phosphate may follow one of two pathways: (i) the pentose phosphates pathway or (ii) glycolysis yielding pyruvate that may be further converted to lactate. In particular, the efflux of glycogen-derived lactate from astrocytes has been associated with brain activation, notably in the scope of memory formation [32,36]. It has also been proposed that lactate may serve as a relevant energy fuel for neurons when energy demands increase [36,41]. However, this so-called lactate shuttle hypothesis [42] would only explain a small fraction of neuronal energy metabolism in the activated brain, with most of the glycogen-derived lactate being released from the brain [32].

4. Brain glycogen and energetic dysfunction in disease

Perturbations of glycogen dynamics may account for brain metabolic dysregulation, compromising normal brain function. Studies in genetically modified mice clearly highlight essential roles of glycogen in the brain: for example, mice lacking glycogen synthase in the brain do not have cerebral glycogen and show hampered performance in memory tasks [34] as well as a higher susceptibility to epilepsy [43]. On the other hand, accumulation of glycogen in neurons may contribute to neurological decline with aging, reproducing features of neurodegenerative diseases [44,45]. In addition, defects in glycogen branching leading to the formation of aggregates inside neurons underlie the most severe form of adolescence-onset epilepsy, Lafora disease [45]. Less prominent alterations of brain glycogen metabolism also contribute to brain energy dysfunction associated with other human diseases, such as epilepsy [46] or diabetes [47], as further discussed in the following paragraphs.

[1] μmol/g is an abbreviation of μmol per gram of wet weight of tissue. The use of μmol/g for living tissue assumes an organ density of ~1000 g/L, which makes μmol/g equivalent to mmol/kg and mM.

In rat models of epilepsy, brain glycogen content was shown to be strongly reduced within a few minutes of continuous seizure activity [48,49]. In a model of chemically-induced seizures, brain glycogen content was shown to increase several hours after seizure activity, presumably playing a role in the resistance to seizures [50]. In humans, glycogen levels in hippocampal biopsies from epileptic patients were found to be higher than those in white and grey matter biopsies [51]. Because this feature was reproduced in healthy pigs, it might reflect differences in regional glycogen distribution, both in pigs and humans [51]. Also in rats, the hippocampus is amongst the brain regions displaying higher glycogen content [16,22,24]. However, brain glycogen accumulation specific to epilepsy would be in agreement with supercompensation following seizure-induced glycogen depletion. In addition, elevated glycogen levels could also energetically sustain neuronal activity during seizures [51]. Taken together, these studies implicate cerebral glycogen in the energetics of seizure activity.

Altered brain glycogen metabolism has also been observed in diabetes. An *in vitro* study found the activity of hexokinase (engaging glucose in glycolysis) reduced whereas those of glycogen phosphorylase and synthase increased in cortical slices of diabetic rats, suggesting glycogen to be a more important fuel than glucose for oxidation in this case [52]. Increased activity of glycogen synthase has also been found in the cortex of type 1 diabetic rats, however without any concentration alterations [53]. These findings indicate that perturbed glycogen metabolism is one key feature of the diabetic brain, not necessarily accompanied by modifications of net glycogen content. Moreover, given the regional differences in brain glycogen content [16,17,22–25], heterogeneity of glycogen metabolism in diabetic brain may be anticipated. For instance, glycogen pools across the brain have been shown to be differently affected by diabetes, *e.g.* reduced glycogen levels were found in the cerebellum of type 2 obese diabetic rats [54], and increased glycogen content was reported in the retina of type 1 diabetic rats [53]. Altered brain glycogen metabolism in diabetes may play an important role in hypoglycemia unawareness, a situation where the blood glucose threshold to elicit a counter-regulatory response is reduced [29,47,55–58]. Glycogen supercompensation could contribute to the development of hypoglycemia unawareness in diabetic patients suffering from recurrent hypoglycemia episodes. However, unlike findings for acute hypoglycemia [29], chronic hypoglycemia induced in rats was not accompanied by brain glycogen supercompensation as assessed *in vivo* by ^{13}C-MRS, but rather by higher brain glucose levels [57]. In line with those studies, a ^{13}C-MRS study in humans also failed to demonstrate glycogen supercompensation in diabetic patients with hypoglycemia unawareness [59], unlike findings in healthy volunteers after a single hypoglycemic episode [37]. By assessing both brain glucose and glycogen contents in rats recovering from acute or chronic hypoglycemia, Herzog et al. [30] found the restoration of brain glucose levels to be faster in the latter case, and to happen together with a more rapid increase in brain glycogen stores, without supercompensation. The authors also confirmed that epinephrine response was blunted in chronic-relative to acute hypoglycemia. Therefore, glycogen supercompensation is not a major contributor to defective counter-regulation in hypoglycemia unawareness, but the latter phenomenon is certainly linked to alterations in the metabolic pathways accounting for glucose-glycogen interconversion in the brain.

5. Non-invasive MR detection of cerebral glycogen

Proton-MRS (^{1}H-MRS) is the most direct method to assess metabolites *in vivo*, since the natural abundance of the ^{1}H isotope is ~100%. The complete visibility of glycogen by ^{1}H-MRS has been demonstrated in solution [60,61]. In the body, the liver is the organ with the highest glycogen content: ~300 μmol/g, as measured in tissue biopsies from human subjects [62]. Glycogen has been observed by ^{1}H-MRS *in vivo* in the liver of humans [63] and mice [64], but this technique fails to account for the totality of hepatic glycogen stores. More precisely, a concentration of ~40 μmol/g was estimated for the human liver [63]. The incomplete visibility of glycogen by ^{1}H-MRS *in vivo* has been attributed to its short spin-spin relaxation time (T_2) [60,65]. This feature hampers glycogen detection by any localized ^{1}H-MRS sequences that make use of echo formation between excitation and acquisition. During the period of the echo formation, an important fraction of glycogen's magnetization is lost due to spin-spin relaxation phenomena, hence becoming unavailable for detection in the course of acquisition. An additional difficulty for ^{1}H-MRS detection of glycogen is that the best resolved ^{1}H resonance of that molecule has a chemical shift of 5.4 ppm, very close to that of water at 4.7 ppm, and is likely affected by the high number of saturation pulses used for suppressing both water and unwanted signals from outside of volume of interest (VOI) in all localized ^{1}H-MRS methods [66,67]. Therefore, quantitative ^{1}H-MRS detection of glycogen remains challenging and even more so in organs with low glycogen content, such as brain.

An alternative approach to ^{1}H-MRS would be chemical exchange saturation transfer MR imaging (CEST MRI), which is sensitive to the interaction of water protons with exchangeable protons in metabolites, such as hydroxyl groups. This technique can thus detect low-concentration metabolites through the saturation of rapidly exchanging protons on these metabolites [68]. CEST MRI has been explored for assessing glycogen content in perfused liver [69] and to some extent in human skeletal muscle [70]. However, the feasibility of these so-called glycoCEST assessments remains to be demonstrated for cerebral glycogen *in vivo*.

Differently from ^{1}H-MRS, the complete visibility of glycogen by ^{13}C-MRS has been demonstrated *in vivo* in the liver [71], skeletal muscle [72] and also brain [58]. In fact, because ^{13}C-MRS sequences applied in the aforementioned studies are essentially pulse-acquire, this technique is suited for compounds with an ultra-short T_2, such as glycogen. Therefore, ^{13}C-MRS is the state-of-the-art technique to assess cerebral glycogen *in vivo* and shares very similar technical challenges with ^{13}C-MRS detection of other carbohydrates, previously reviewed by, *e.g.*, Gruetter et al. 2003 and de Graaf et al. 2011 [73,74], and in this issue as well. Nonetheless, specific properties of brain glycogen make it worth highlighting how its detection by ^{13}C-MRS *in vivo* benefits from a careful optimization of technical settings and experimental parameters. First and foremost, the amount of naturally occurring ^{13}C atoms in brain glycogen is very low. The ^{13}C isotope of carbon displays a natural abundance of 1.11% and, since glycogen was found in the range of 3–10 μmol/g in the human and rodent brain [15–21], this yields that only 0.03–0.1 μmol/g can be detected by ^{13}C-MRS *in vivo*. In addition, the unique physical properties of glycogen: ultra-short T_2 and comparable spin-lattice relaxation time (T_1, see Table 1), have to be taken into consideration when selecting and developing the technical tools for its ^{13}C-MRS detection. Specially, echo-based localization methods are not practicable for measuring cerebral glycogen *in vivo*.

In the following sections, we will focus on strategies to improve the sensitivity of ^{13}C-MRS detection of glycogen C1. Firstly, we explore the benefits arising from technical development of both hardware and MR sequence design. And lastly, we discuss the experimental approach of brain glycogen studies *in vivo* that currently relies on the administration of exogenous ^{13}C-enriched glucose precursors to increase the detected ^{13}C-1 signal of glycogen.

Table 1
T_1 and $T_2/T_2^*/T_{2app}$ for ^{13}C1 glycogen.

B_0 (T)	T_1 (ms)	$T_2/T_2^*/T_{2app}$ (ms)	Temperature (°C)	References
2.1	220 ± 10	11–31.1	27	Sillerud LO and Shulman RG 1983 [109]
	65 ± 5	6.7 ± 1	22	Zang L et al., 1990 [110]
4.7	162 ± 6	7.3[a]-15.1[b]	37	Overloop K et al., 1996 [111]
	158 ± 15*	5 ± 2*	37	Zang L et al., 1990 [110]
	142 ± 10	9.4 ± 1	22	Zang L et al., 1990 [110]
		5*[,d]	37	Gruetter R et al., 1994 [71]
8.4	304 ± 5	7.8[a]-13.3[b]	37	Overloop K et al., 1996 [111]
	310 ± 10	13 ± 2	37	Zang L et al., 1990 [110]
	300 ± 10	9.5 ± 1	22	Zang L et al., 1990 [110]
9.4	332 ± 15*	6.6 ± 1.1*[,d]	37	Van Heeswijk RB et al., 2012 [78]
	340 ± 10[c]	N/D	37	Choi IY et al., 2000 [80]
	330 ± 30*	N/D	37	Choi IY et al., 2000 [80]
14.1	521 ± 34*	5.9 ± 1.0*[,d]	37	Van Heeswijk RB et al., 2012 [78]

[a,b] 11.1 mM glycogen ^{13}C1.
"*"measurements *in vivo*.
N/D not detected.
[a] ^{13}C1-α and.
[b] ^{13}C1-β
[c] 400 mM natural abundance oyster glycogen (4.4 mM glycogen^{13}C1).
[d] Estimated from the spectral linewidth.

6. Technical features of ^{13}C-MRS of cerebral glycogen

6.1. Effect of higher magnetic fields (B_0)

Sensitivity is known to be enhanced with the increase of magnetic field strength (B_0), *i.e.* signal-to-noise ratio (SNR) ∝ B_0^β [13,21,37,59,75–77]. In theory, when the sensitivity exclusively depends on B_0, the signal increases with B_0^2 ($\beta = 2$). However in practice, β falls in the range of 1–1.75 due to noise arising from electric hardware components, the sample itself, or other random sources. Consequently, with β~1, the sensitivity increases linearly with B_0. Thus, at high fields, the acquisition time required to achieve SNR levels similar to those obtained at lower fields can be shortened, as shown for ^{13}C-MRS detection of glycogen C1 at 14.1 T *vs*. 9.4 T [78].

6.2. Radio-frequency (RF) coil design

Design of the RF coil (see reviews from Magill and Gruetter [79], and Ipek in the current issue) can be tailored to improve detection of glycogen ^{13}C-1 by providing high sensitivity at the ^{13}C frequency without exceeding the specific absorption rates (SAR) limits at the ^{1}H frequency when using ^{1}H decoupling. This feature is critical when developing a coil for ^{13}C-MRS since decoupling is commonly used to improve ^{13}C signal detection (see discussion below) and SAR limits are highly restricted for human applications, even more so at ultra-high magnetic field.

In general terms, a typical ^{13}C-MRS experiment requires a double tuned ^{13}C–^{1}H transceiver coil, in which the ^{13}C-coil detects ^{13}C signals and the ^{1}H-coil is used for: (i) anatomical imaging for precise placement of VOI; (ii) adjusting field inhomogeneity; (iii) decoupling J_{CH}-coupling. For instance, ^{13}C-linear coils (*i.e.* single ^{13}C loop) in combination with ^{1}H-quadrature coils (*i.e.* two physically-decoupled overlapped ^{1}H loops) have been widely used both in animal [18,29,57,58,78,80,81] and human studies [21,76,77,82]. Relative to the linear coil design, an overlapped quadrature coil enhances sensitivity by a factor of $\sqrt{2}$ [79,83], and ^{13}C-quadrature coils have been designed in combination with either a ^{1}H-volume coil [84] or a ^{1}H-quadrature coil [85]. Indeed, an SNR enhancement of nearly $\sqrt{2}$ has been achieved to detect glycogen ^{13}C-1 *in vivo* at 7 T with the latter design when comparing to the linear-^{13}C/quadrature-^{1}H coil [85].

Besides coil design, it is also crucial to eliminate any unwanted noise introduced in the paths of RF chains, which can be afforded by inserting bandpass (^{1}H pass, ^{13}C stop)/lowpass (^{13}C pass, ^{1}H stop) filters in between the corresponding paths of RF chains [73,74,79].

6.3. Decoupling

Most carbons of biomolecules, including glycogen, are directly bonded to protons and experience J_{CH}-coupling, which splits ^{13}C signals into multiplets. The ^{1}H-coil can offer efficient decoupling, collapsing the multiplets into singlets, simplifying the ^{13}C spectra and effectively increasing the sensitivity [86].

Decoupling relies on the use of RF pulses that, like excitation pulses delivered by the ^{13}C-coil, also contribute to the SAR. Even though the decoupling RF pulses have been developed towards increasing decoupling bandwidth without exceeding the SAR for human applications, most ^{13}C-MRS applications on brain glycogen have relied on a low-power broadband WALTZ-16 decoupling scheme [86], which can be shortened [76,80,85,87] in adaptation to the very short T_2 of glycogen C-1 (Table 1). Nevertheless, in most brain glycogen measurements by ^{13}C-MRS, there is also an interest in assessing brain glucose signals and, for this, longer duration RF decoupling pulses are anticipated.

6.4. Field inhomogeneity

The typical spectral full width at half maximum (FWHM) of a given resonance is equal to $1/\pi T_2$, and becomes $1/\pi T_2^*$ when the influence of field inhomogeneity ($\gamma\Delta B_0$) is taken into account, i.e. $1/T_2^* = 1/T_2 + \gamma\Delta B_0$. The effect of field inhomogeneity ($\gamma\Delta B_0$) on the FWHMs of ^{13}C resonances is reduced four-fold compared to that observed for ^{1}H resonances due to $\gamma_{13C}/\gamma_{1H} = 0.25$ [74]. Nonetheless, the influence of field inhomogeneity on ^{13}C resonances becomes substantial especially when large VOIs in combination of high magnetic fields are commonly used for ^{13}C-MRS detection of glycogen, in benefit of improved sensitivity. Taking the example of a $(8 \times 5 \times 5)$ mm^3 volume, typically used for ^{13}C MRS measurement of cerebral glycogen in rats, improving field homogeneity with shimming may reduce the linewidth of the water ^{1}H resonance from 126 Hz to 15 Hz at 9.4 T, *i.e.* yielding a reduction of 111 Hz (0.28 ppm), as experimentally measured in our system. A more pronounced effect of shimming was observed for our 14.1T system: the linewidth of water ^{1}H resonance was reduced from 580 Hz to 22 Hz, *i.e.* yielding a reduction of 558 Hz (0.9 ppm). Considering a

Lorenzian spectral line shape, the signal amplitude (I) is proportional to $\frac{1}{FWHM}$ and thus the signal amplitude change can be estimated as $\frac{I}{I^*} = \frac{FWHM^*}{FWHM}$, in which I* and FWHM* stand for signal amplitude and linewidth without any shimming compensation, respectively. Therefore, taking the example at 14.1 T, a reduction of 558 Hz on the linewidth of the water ^{1}H signal translates into a 24-fold increase of the water signal amplitude. Such field inhomogeneity is expected to induce a 140 Hz widening effect on the FWHM of ^{13}C MR spectra since $\gamma_{13C}/\gamma_{1H} = 0.25$ ($1/T_2^* = 1/T_2 + \gamma_{13C}\Delta B_0$). When the FWHM of glycogen ^{13}C-1 is 64 Hz at 14T (*i.e.*, FWHM $= 1/\pi T_2$ with $T_2 = 5$ ms, Table 1), the field inhomogeneity may enlarge the FWHM* of glycogen ^{13}C-1 resonance to ~200 Hz, and consequently induces a >3-fold reduction of its amplitude.

Overall, shimming minimizes field inhomogeneity and thus increases T_2^*, translating into narrowing linewidth and increasing signal amplitude. The need of adjusting shim coils becomes important, especially at ultra-high magnetic fields.

6.5. Localization

Spatial localization defines the VOI and is essential for reliable non-invasive detection of cerebral ^{13}C-glycogen. In particular, non-echo based localization methods are desired to define a 3D volume within the brain tissue, given the ultra-short T_2 of glycogen (Table 1).

6.5.1. Chemical shift imaging (CSI)

Chemical shift imaging (CSI) is one approach to perform localization in MRS [88,89]. For instance, 1D CSI requires an additional phase-encoding gradient to define spatial localization and has been applied for liver glycogen detection by ^{13}C-MRS in humans [89].

Many approaches have been pursued to shorten the acquisition time for CSI whilst maintaining the desired sensitivity, *e.g.* using a sampling k-space scheme [90]. Alternatively, Fourier series window (FSW) became useful for the development of surface coil rotating frame experiments, which depend on an inhomogeneous B_1 field gradient for excitation [91,92]. However, the dephasing step in the FSW is not as efficient as single-voxel localization spectroscopy. For instance, the SNR per time unit in the FSW approach in detection of ^{13}C glycogen was ~30% less than that of single-voxel ^{13}C-MRS studies [93]. In addition, the Fourier transform reconstruction can lead to intervoxel signal contamination from the very nearby extracerebral glycogen due to point spread function effects. Therefore, single-voxel localization remains the preferred method for ^{13}C-MRS detection of glycogen in brain, as discussed in the following paragraphs.

6.5.2. Image-selected In vivo spectroscopy (ISIS)

This method explores the slice-selective principle of MRI techniques for localizing MR signals from a specific volume, as suggested by Ordidge and coworkers [94], and has been applied for ^{13}C-MRS detection of liver glycogen in humans [95]. The technique is based on a slice-selective inversion of spins prior to their excitation and signal acquisition. More specifically, to obtain an MR signal from a given slice, two scans are required. In the first, the free induction decay (FID) is obtained with all the spins in the volume having the same phase; in the second, the FID is acquired in the same way except that spins in the target slice are first inverted using a slice selective 180° pulse. When the two FIDs are subtracted, only the signal from the target slice remains. The 3D volume can be localized using linear combinations of such scheme in three directions and a minimum number of eight scans is necessary for canceling out unwanted signals from outside the target volume.

One advantage of this method is the absence of T_2 weighting, since there is no echo time in this pulse sequence. However, ISIS relies on inverting spins in the VOI, which can result in signal loss due to T_1 of glycogen and imperfect slice profiles. An additional caveat of the add-subtract scheme of ISIS is that it makes localization vulnerable to any subtraction errors related to motion or RF pulse imperfections.

6.5.3. Outer volume suppression (OVS)

Instead of exciting the spins in the VOI, the slice-selective schemes with 90° nominal pulses can be applied to destroy magnetization outside the VOI by flipping it into the transverse plane and dephasing it with spoiler gradients, so that no net magnetization outside the VOI remains [66]. In brief, to localize one dimension, two suppression slices must be placed at both sides of the VOI and a 3D volume may be defined using three pairs of OVS pulses. The frequencies of the paired slice-selective pulses are placed in the center of the suppression slices instead of the center of the target VOI. Once three pairs of suppression slices are properly positioned and the pulses are applied, a localized MR spectrum can be acquired by using a simple non-selective excitation RF pulse. The selected pair or the entire OVS module can be repeated several times, to ensure a robust suppression of the surrounding magnetization.

Similar to ISIS, OVS also allows data acquisition immediately after the non-selective excitation RF pulse, an advantageous feature for obtaining accurate signals from metabolites with short T_2, such as glycogen (Table 1). In addition, OVS can achieve localization in one scan and is, therefore, resistant to motion and system instability.

It is clear that suppression is the key element to ensure localization and must be extremely efficient to avoid contamination from outside of the VOI. The thickness of the different suppression slices depends on the placing of the VOI within the coverage of the coil, and is not necessarily the same for every slice. With increasing subject size and decreasing VOI size, OVS can be very challenging since strong signals from the outer volume need to be suppressed, which requires RF pulses with large bandwidths and high amplitudes.

OVS *per se* is usually not efficient enough to obtain clean MR spectra [66] and is, therefore, used in combination with other localization techniques, as addressed in the following paragraph for the case of brain glycogen.

6.5.4. Localized ^{13}C-MRS detection of brain glycogen in practice

To achieve high ^{13}C sensitivity with low ^{1}H power deposition, the linear-^{13}C coil in combination with the quadrature-^{1}H coil design has been widely used for rodent [80,86,96] and human studies [21,82,95,97]. As a result, a 3D localization method of ^{13}C glycogen adapted to that coil design was developed. This method was initially developed for the rodent brain and is based on a T_1-optimized OVS scheme [80,96]. In order to detect the sensitive volume of the ^{13}C coil, reduce B_1 and signal variations perpendicular to B_0 and the ^{13}C coil ("x" axis, horizontal, Fig. 1), and minimize contamination from skeletal muscle glycogen, a slice-selective inversion recovery unit is applied. When the inverted magnetization of glycogen from the skeletal muscle right beside the VOI approaches zero (inversion recovery delay time according to T_1 of glycogen ^{13}C-1), six nominal 90° pulses are applied on the slices parallel to the VOI to minimize the residual z-magnetization (Fig. 1B). Due to the usage of the ^{13}C-linear surface coil, the performance of the OVS perpendicular to the RF coil and B_0 ("y" axis, vertical, Fig. 1) is compromised. Therefore, an additional 1D ISIS with corresponding phase cycling is applied in conjunction with a y-slice gradient containing the VOI (Fig. 1B).

After the OVS-ISIS localization modules, an adiabatic half-

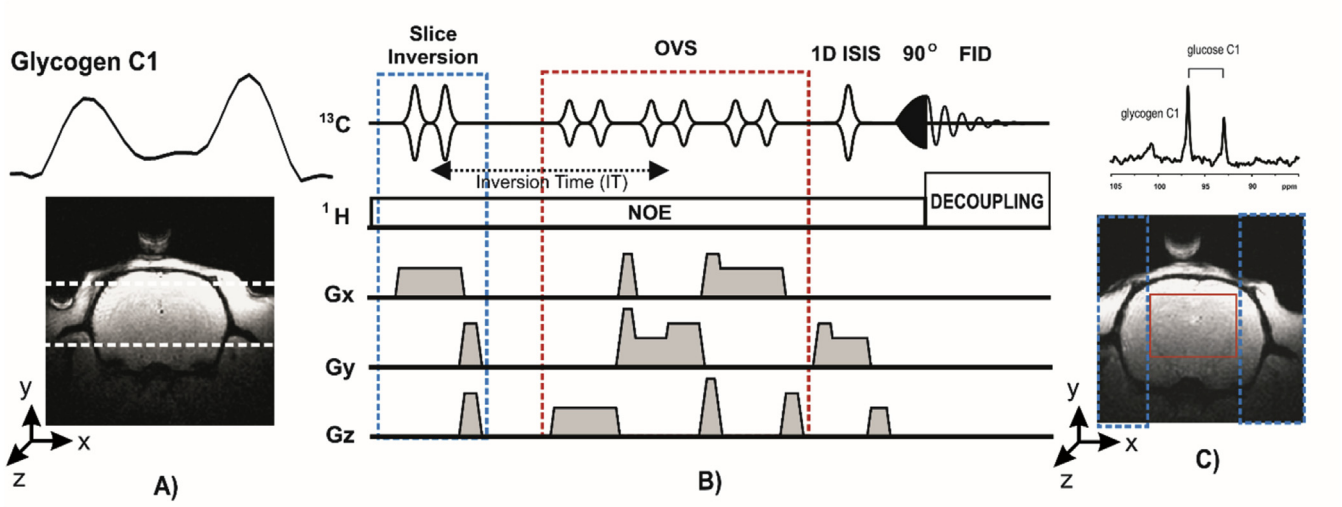

Fig. 1. Improvements of a pulse sequence for ^{13}C-MRS detection of glycogen in the rat brain. A) After a 4 h infusion of 20% w/v [1–^{13}C]glucose, a project profile of glycogen ^{13}C-1 (99–102 ppm) between two dashed lines with 1D CSI approach [89] shows that glycogen signals arise from skeletal muscle. B) A typical 3D localization ^{13}C MRS pulse sequence diagram for ^{13}C detection of glycogen in the rat brain [80,96]. The localization performance for glycogen ^{13}C-1 is ensured by applying (ii) a slice inversion unit (blue dashed squares in B and C); (ii) a 3D OVS unit (red dashed square, an inversion time is optimized for nulling z-magnetization from extracerebral glycogen); and (iii) 1D ISIS on y-axis. Glycogen ^{13}C-1 signal is further enhanced by (i) an adiabatic excitation 90° pulse to increase the excitation volume; and (ii) bi-level WALTZ-16 RF pulses on ^{1}H channel during excitation for NOE and during signal acquisition for decoupling J_{CH}. C) Once a 3D volume (red square) is defined by the localized ^{13}C MRS, glycogen ^{13}C-1 and glucose ^{13}C-1 can be obtained from rat brain after the administration of [1–^{13}C] glucose.

passage 90° pulse is used for excitation immediately followed by acquisition of the FID. In addition, bi-level WALTZ-16 RF pulses [86] are applied to the proton channel, enhancing the sensitivity of ^{13}C-1 glycogen detection in two ways: (i) via nuclear Overhauser effect (NOE) that transfers magnetization from protons to glycogen ^{13}C-1 during excitation; and (ii) affording decoupling of J_{CH}-coupling during the signal acquisition period.

Due to the use of the ^{13}C-linear surface coil, whose size is actually smaller than that of the entire brain, it is desired that all RF pulses used for inversion, saturation and excitation are adiabatic [80,96]. For instance, the advantages of nominal adiabatic 90° hyperbolic secant pulses used for OVS [98] are (i) to be tailored to meet the specific needs of the *in vivo* geometry within the RF power limits, (ii) to provide a B_1-insensitive slice selection profile and (iii) to minimize chemical shift displacement errors through broad bandwidth of the pulse. In the case of excitation and inversion, the adiabatic pulse, above a certain B_1 threshold, offers the same nutation independent of B_1 amplitude and is beneficial for a large VOI [96,98].

The overall method initially developed for studies of the rodent brain was modified and optimized to be applied to humans. Specifically, in the latter case and unlike for the rodent brain, there is no surrounding skeletal muscle to potentially contaminate the VOI with extracerebral glycogen. Therefore, no slice-selective recovery module is included in the ^{13}C-MRS sequences used for human studies of brain glycogen [21,76].

7. Experimental aspects of ^{13}C-MRS of cerebral glycogen

7.1. Quantification of cerebral glycogen detected by ^{13}C MRS

To obtain quantitative information from ^{13}C-MR spectra acquired *in vivo*, glycogen ^{13}C-1 signal is converted to concentration. Internal reference methods are often the choice for quantification in ^{1}H-MRS, where a standard compound measured in the spectrum (*e.g.* creatine) or tissue water are used for scaling. However, these methods are not applicable to ^{13}C-MRS of cerebral glycogen due to the absence of a natural abundance ^{13}C signal from any highly concentrated compound in the brain. An alternative option is to reproduce ^{13}C-MRS measurements *in vivo* on a phantom containing an aqueous glycogen solution of known concentration, the so-called external reference method [71]. To accurately perform this method, a reference ^{13}C signal from a ^{13}C-enriched compound (*e.g.* formic acid in a closed sphere) should be provided at the ^{13}C coil for corrections related with coil performance, such as loading or adjustments of transmitting and receiving powers [71,97]. Other factors, including T_1, T_2 and NOE, have to be taken in to account between the external reference phantom solution and *in vivo* scans. In addition, some imperfections can be corrected by the external reference method, namely off-resonances effects [74]. As mentioned in the previous section, the intrinsic characteristic of the applied adiabatic half passage pulses for excitation is to offer the same nutation flip angles (*e.g.* 90° is desired for a maximal excitation for detection of glycogen ^{13}C-1) independent of B_1 amplitude when the carrier frequency of the pulse is equal to the Lamar frequency of spins of the target metabolite, so called on-resonance. This feature is often accompanied by non-uniform RF excitation profiles away from the carrier frequency of the excitation pulse, *i.e.* off-resonance [99–101]. Therefore, adjacent metabolites are affected by a possible sub-maximal excitation, so called off-resonance effects. For instance, when studies measure both glucose and glycogen ^{13}C-1 signals with the carrier frequency on the resonance near glycogen ^{13}C-1 (100.5 ppm), an accurate quantification of both molecules from their ^{13}C signals has to consider the extent to which such off-resonance effects impact the nearby glucose ^{13}C-1 signals (96.8 and 93.2 ppm) [102]. The effects can be reproduced in phantoms of known glycogen and glucose concentrations, thereby allowing to correct the data acquired *in vivo*.

7.2. Administration of ^{13}C-enriched glucose

The administration of ^{13}C-labeled precursors (typically [1–^{13}C] glucose) is essential to enrich the brain glycogen pool with ^{13}C to levels detectable by ^{13}C-MRS *in vivo*. This experimental strategy not only facilitates glycogen quantification, as it also allows to follow

^{13}C-label incorporation into glycogen carbons in real time, when the glucose precursor is continuously delivered to the blood stream. With this approach, ^{13}C-MRS becomes a very insightful technique to characterize cerebral glycogen metabolism in animals and humans *in vivo* (recently reviewed by Khowaja A et al., 2015 [2]). The rationale behind tracer[2] studies of brain glycogen metabolism is explored in the following paragraphs, with examples from published studies in rats and humans.

There are two approaches to enrich cerebral glycogen with ^{13}C from ^{13}C-labeled glucose: (i) by continuous infusion of the labeled precursor [57,58,77,80,96]; or (ii) with extensive pre-labeling by *ad-libitum* ingestion [18]. Both methods have been combined to study brain glycogen kinetics in rats after a 24 h pre-labeling period, when complete turnover[3] of the brain glycogen pool is achieved [81,93].

7.2.1. Isotopic enrichment and glycogen content

In studies using ^{13}C-labeled precursors, isotopic enrichment of both precursor and product should be characterized for an accurate and comprehensive interpretation of metabolic fluxes [103]. In the case of glycogen kinetics, this means assessing the isotopic enrichment of both glycogen and glucose in the brain.

Upon administration of a^{13}C-glucose tracer, its isotopic enrichment will be diluted by endogenous unlabeled glucose, essentially from hepatic glucose production. As a result, the isotopic enrichment of brain glucose, available for glycogen synthesis, will be well below that of the administered tracer. This effect can be minimized under a continuous glucose infusion by co-infusing insulin, which limits hepatic production of unlabeled glucose. Given the rapid equilibration of glucose across the blood brain barrier [57] [104–106], isotopic enrichment of arterial glucose is essentially that of brain glucose, what has been confirmed in brain extracts in rats [81]. Hence, the ^{13}C enrichment of plasma glucose may be used as a surrogate of that of brain glucose, an assumption relevant for human studies [21,37,59].

Assessing the isotopic enrichment of glycogen is the only way to verify whether the pool has been completely turned over and also to obtain the total concentration of glycogen (both ^{13}C and ^{12}C). In animal experiments, the isotopic enrichment of brain glycogen can be determined directly in tissue extracts [58]. In addition, determination of brain glycogen isotopic enrichment has been afforded by using N-acetyl-aspartate as a reporter molecule in the rat brain *in vivo* [18]. Importantly, this method has been validated in rats against *in vitro* measurements in tissue extracts [81]. In humans, non-invasive assessments of brain glycogen isotopic enrichment remain to be demonstrated.

The isotopic enrichment of glycogen is dependent on the isotopic enrichment of brain glucose and glycogen metabolic turnover, as illustrated in Fig. 2. For example after 1–2 days pre-labeling [81], the isotopic enrichment of glycogen was similar to that of brain glucose, indicating complete glycogen turnover, but below that of glucose in the drinking water, due to dilution by endogenous glucose production. In contrast, when 99% [1–^{13}C]glucose was continuously infused to maintain moderate hyperglycemia over several hours [58], the isotopic enrichment of brain glucose (~90%) was close to that of the infusate but the isotopic enrichment of glycogen was significantly lower (~77%). Therefore, the latter findings denote negligible dilution from endogenous glucose production but non-complete glycogen turnover.

7.2.2. Glycogen synthesis, breakdown and turnover by ^{13}C MRS

The brain glycogen pool reflects the activity of enzymes with opposite effects: glycogen synthase (adding glucosyl units to glycogen) and glycogen phosphorylase (removing glucosyl units from glycogen). Because the activities of both enzymes occur simultaneously, increases in glycogen ^{13}C-1 following the infusion of [1–^{13}C]glucose may denote simple turnover (accumulation of ^{13}C-glycogen without changes in total concentration) and/or net synthesis (effective increase in total glycogen concentration). The relative contribution of each of those phenomena will depend on the experimental and pathophysiological conditions. For example, with 48 h pre-labeling Choi and Gruetter [18] found total brain glycogen concentration to be ~3 μmol/g. Comparatively, after 4 h of [1–^{13}C]glucose infusion (set to maintain glycemia at 13–16 mM), brain ^{13}C-glycogen alone was substantially higher, amounting to 5 μmol/g [80], and even more so when glucose infusion was preceded by an hypoglycemic period inducing supercompensation [29,58]. Taken together, these studies support the notions that net glycogen synthesis may take place in the brain under certain conditions such as hyperglycemia and supercompensation.

Resolving synthase and phosphorylase fluxes from net synthesis is possible by ^{13}C-MRS *in vivo* with appropriate glucose infusion tracers and protocols. Valuable kinetic information on enzymatic fluxes is achieved when label incorporation (or disappearance) into glycogen ^{13}C-1 is followed and glycogen concentration is at steady-state, *i.e.* no net synthesis (or degradation) [107]. For example, when infusing [1–^{13}C]glucose, changes in glycogen ^{13}C-1 signal report synthase flux, and conversely when switching the infused solution to unlabeled glucose the decrease of glycogen ^{13}C-1 reflects phosphorylase flux. In such pulse-chase experiments, glycogen turnover rate has been estimated in rats to be ~0.5 μmol $g^{-1}.h^{-1}$, with presumably minimal net glycogen synthesis [80,96]. A similar rate of ~0.7 μmol $g^{-1}.h^{-1}$ was found when the contribution of net synthesis was ruled out, by infusing [1,6–$^{13}C_2$]glucose at an isotopic enrichment matching that of glycogen achieved with [1–^{13}C]glucose during a pre-labeling period [93]. Therefore, brain glycogen turnover in rats is very slow, with a turnover time[4] of ~8 h [80,93,96].

On the other hand, achieving an isotopic stead-state where no changes are observable on glycogen ^{13}C-1 due to a constant isotopic enrichment over time, is a pre-requisite to investigate the effect of specific conditions (such as variations in insulin or glucose levels, for instance) on brain glycogen mobilization. Isotopic steady-state of brain glycogen has been accomplished by means of a pre labeling period in rats [81,93] or after prolonged infusion of >5 h in rats [29] and >48 h in humans [77].

When the above mentioned methodological considerations are acknowledged, very insightful information on cerebral glycogen kinetics is achieved. Namely, rodent ^{13}C-MRS studies *in vivo* showed that glycogen consumption in the brain increases upon insulin-induced hypoglycemia and that, when normoglycemia is restored, glycogen synthesis takes place and supercompensation occurs [29]. Such studies also indicate that, when sufficient glucose is present, insulin mainly promotes glycogen turnover rather than net synthesis [81].

[2] ^{13}C-labeled precursors used to follow given metabolic pathways are actually administered at doses that largely surpass tracer amounts to improve sensitivity of ^{13}C-MRS detection. For instance, isotopic enrichment of [1–^{13}C]glucose used as a precursor for brain glycogen in ^{13}C-MRS studies *in vivo* ranges from 25% (in humans) to 99% (in rats).

[3] Refers to the rate at which glucosyl units in glycogen are replaced by new ones, derived from the administered tracer, via simultaneous synthesis and breakdown. Complete turnover means that all the glucosyl units have been replaced, which yields that the glycogen pool exists at isotopic and metabolic steady state.

[4] Turnover time is the time required for all the glycogen to be replaced by newly synthesized molecules at a given rate, and is given by the ratio between the pool size (in μmol/g) and the metabolic or turnover rate (in $\mu mol.g^{-1}.h^{-1}$) [18].

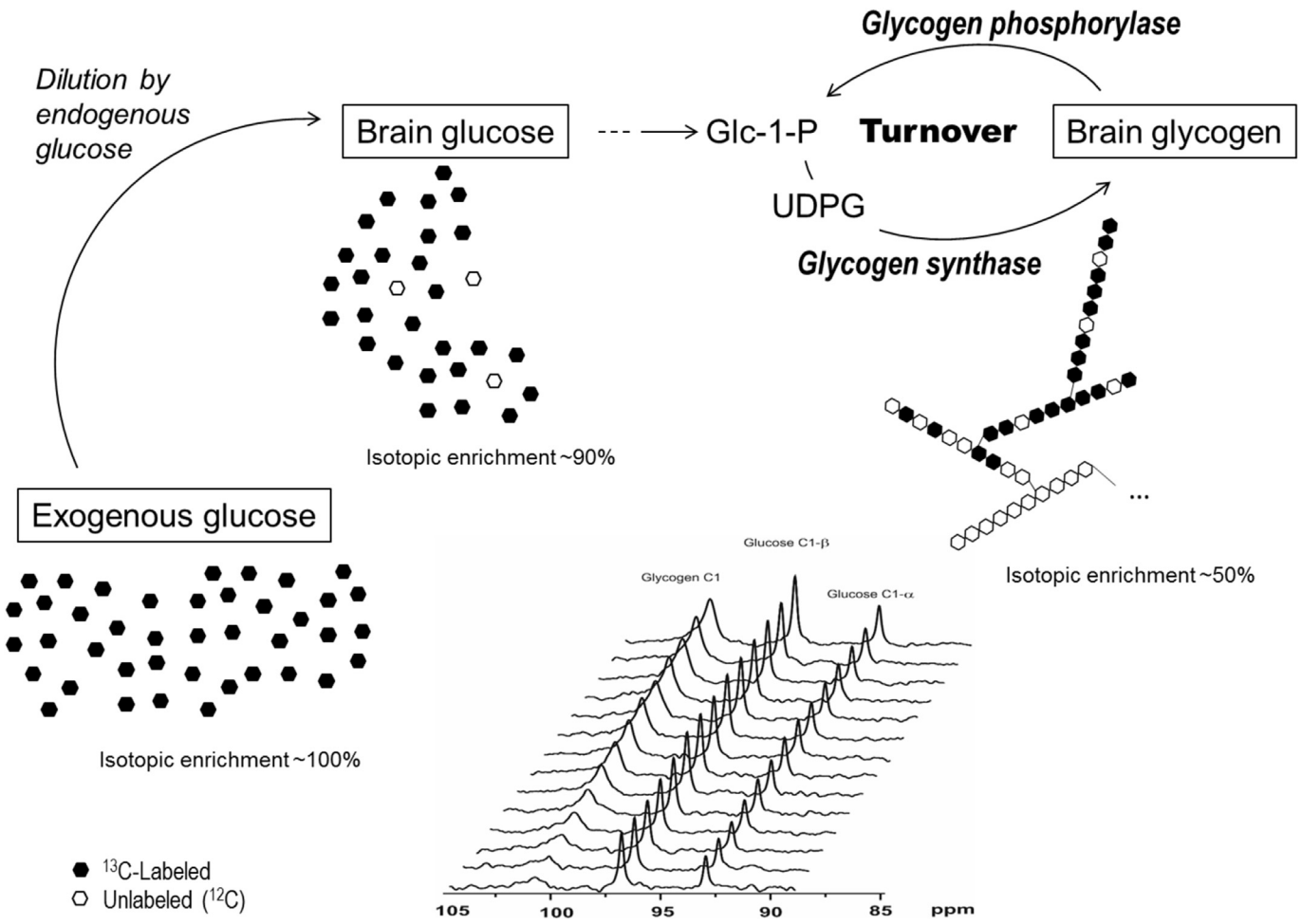

Fig. 2. Depiction of glycogen labeling from exogenous ^{13}C-labeled glucose and example spectra of brain glucose and glycogen acquired by ^{13}C-MRS *in vivo*. Once in the body, the isotopic enrichment of the administered solution (infused or ingested) is diluted by endogenous unlabeled glucose, and the isotopic enrichment of brain glucose will be reduced in proportion to that contribution. With time, glycogen becomes progressively labeled as the simultaneous activities of glycogen synthase and phosphorylase replace unlabeled glucosyl units by ^{13}C-labeled ones via the phosphorylated intermediates glucose-1-phosphate (Glc-1-P) and uridine diphosphate glucose (UDPG). Glycogen turnover is complete when its isotopic enrichment reaches that of the precursor glucose pool at isotopic steady-state. The figure illustrates incomplete turnover, commonly observed in the first few hours of infusion studies. Changes in brain glucose and glycogen ^{13}C-1 signals can be followed over time by localized ^{13}C-MRS *in vivo*, as shown in the stacked ^{13}C spectra (adapted from the study by Lei et al., 2007 [58]).

Despite the absence of direct validation, in humans, brain glycogen turnover has been modeled with some assumptions, yielding a synthesis flux of 0.16–0.28 μmol $g^{-1}.h^{-1}$, with turnover times in the range of days [21,37,59]. Hence, brain glycogen metabolism is slower in humans, relative to that of rats. When glycogen ^{13}C-1 data were fitted with a biophysical model accounting for synthase and phosphorylase activities at the level of the individual glucose chain [108], glycogen content in the healthy human occipital lobe was estimated to be ~8 μmol/g [75]. This finding is in close agreement with values determined by ^{13}C-MRS *in vivo* in the rodent brain.

In a recent ^{13}C-MRS study *in vivo*, Öz et al. were able to detect alterations in brain glycogen metabolism in diabetic patients, who displayed lower levels of newly synthesized glycogen relative to healthy volunteers, a finding that may indicate reduced brain glycogen levels and/or slower turnover in diabetic patients [59].

8. Concluding remarks

To date, ^{13}C-MRS remains the state-of-the-art technique to assess cerebral glycogen and its metabolism *in vivo*. Despite the challenges in technical development and biological interpretations, this method has provided valuable insights into brain glycogen content and kinetics. So far, the potential of MRS to characterize brain glycogen metabolism in disease has been addressed in type-1 diabetic patients, with limited but promising results. Therefore, fully elucidating cerebral glycogen metabolism *in vivo* in pathological conditions remains to be explored and can strongly benefit from rodent studies that allow for direct validation.

Acknowledgements

The authors are grateful to Drs. João M. N. Duarte & Eulalia Serés Roig for their constructive comments and insightful discussion during the preparation of the manuscript. Supported by the Centre d'Imagerie BioMédicale of the UNIL, UNIGE, HUG, CHUV, EPFL and the Leenaards and Louis-Jeantet Foundations.

References

[1] A.D. Baron, et al., Rates and tissue sites of non-insulin- and insulin-mediated glucose uptake in humans, Am. J. Physiol-Endoc M. 255 (6) (1988) E769–E774.
[2] A. Khowaja, et al., *In vivo* Magnetic Resonance Spectroscopy of cerebral glycogen metabolism in animals and humans, Metab. Brain Dis. 30 (1)

(2015), p. 255–261.
[3] R. Meléndez, E. Meléndez-Hevia, M. Cascante, How did glycogen structure evolve to satisfy the requirement for rapid mobilization of glucose? A problem of physical constraints in structure building, J. Mol. Evol. 45 (4) (1997) 446–455.
[4] Z. Gunja-Smith, et al., A revision of the Meyer-Bernfeld model of glycogen and amylopectin, FEBS Lett. 12 (2) (1970) 101–104.
[5] J. Shearer, T.E. Graham, Novel aspects of skeletal muscle glycogen and its regulation during rest and exercise, Exerc. Sport Sci. Rev. 32 (3) (2004) 120–126.
[6] E. Meléndez-Hevia, T.G. Waddell, E.D. Shelton, Optimization of molecular design in the evolution of metabolism: the glycogen molecule, Biochem. J. 295 (2) (1993) 477–483.
[7] M.D. Alonso, et al., A new look at the biogenesis of glycogen, FASEB J. 9 (12) (1995) 1126–1137.
[8] A. Philp, M. Hargreaves, K. Baar, More than a store: regulatory roles for glycogen in skeletal muscle adaptation to exercise, Am. J. Physiol. Endocrinol. Metabol. 302 (11) (2012) E1343–E1351.
[9] K.K. Rybicka, Glycosomes — the organelles of glycogen metabolism, Tissue Cell 28 (3) (1996) 253–265.
[10] Q.A. Besford, et al., The structure of cardiac glycogen in healthy mice, Int. J. Biol. Macromol. 51 (5) (2012) 887–891.
[11] P.O. Powell, et al., Acid hydrolysis and molecular density of phytoglycogen and liver glycogen helps understand the bonding in glycogen α (composite) particles, PLoS One 10 (3) (2015) e0121337.
[12] M.A. Sullivan, et al., Changes in glycogen structure over feeding cycle sheds new light on blood-glucose control, Biomacromolecules 15 (2) (2014) 660–665.
[13] M.A. Sullivan, et al., Molecular structural differences between type-2-diabetic and healthy glycogen, Biomacromolecules 12 (6) (2011) 1983–1986.
[14] R. Gruetter, Glycogen: the forgotten cerebral energy store, J. Neurosci. Res. 74 (2) (2003) 179–183.
[15] S.R. Nelson, et al., Control of glycogen levels in brain, J. Neurochem. 15 (11) (1968) 1271–1279.
[16] R.A. Swanson, Physiologic coupling of glial glycogen metabolism to neuronal activity in brain, Can. J. Physiol. Pharmacol. 70 (Suppl) (1992) S138–S144.
[17] J. Kong, et al., Brain glycogen decreases with increased periods of wakefulness: implications for homeostatic drive to sleep, J. Neurosci. 22 (13) (2002) 5581–5587.
[18] I.Y. Choi, R. Gruetter, *In vivo ^{13}C NMR assessment of brain glycogen concentration and turnover in the awake rat*, Neurochem. Int. 43 (4–5) (2003) 317–322.
[19] F.D. Morgenthaler, et al., Biochemical quantification of total brain glycogen concentration in rats under different glycemic states, Neurochem. Int. 48 (6–7) (2006) 616–622.
[20] N.F. Cruz, G.A. Dienel, High glycogen levels in brains of rats with minimal environmental stimuli: implications for metabolic contributions of working astrocytes, J. Cereb. Blood Flow. Metab. 22 (12) (2002) 1476–1489.
[21] G. Oz, et al., Direct, noninvasive measurement of brain glycogen metabolism in humans, Neurochem. Int. 43 (4–5) (2003) 323–329.
[22] R.A. Swanson, S.M. Sagar, F.R. Sharp, Regional brain glycogen stores and metabolism during complete global ischaemia, Neurol. Res. 11 (1) (1989) 24–28.
[23] J. Garriga, M. Sust, R. Cusso, Regional distribution of glycogen, glucose and phosphorylated sugars in rat brain after intoxicating doses of ethanol, Neurochem. Int. 25 (2) (1994) 175–181.
[24] T. Matsui, et al., Brain glycogen decreases during prolonged exercise, J. Physiol. (Lond) 589 (Pt 13) (2011) 3383–3393.
[25] S.M. Sagar, F.R. Sharp, R.A. Swanson, The regional distribution of glycogen in rat brain fixed by microwave irradiation, Brain Res. 417 (1) (1987) 172–174.
[26] C.H. Phelps, Barbiturate-induced glycogen accumulation in brain. An electron microscopic study, Brain Res. 39 (1) (1972) 225–234.
[27] D. Vilchez, et al., Mechanism suppressing glycogen synthesis in neurons and its demise in progressive myoclonus epilepsy, Nat. Neurosci. 10 (11) (2007) 1407–1413.
[28] T. Matsui, et al., Brain glycogen supercompensation following exhaustive exercise, J. Physiol. (Lond) 590 (Pt 3) (2012) 607–616.
[29] I.Y. Choi, E.R. Seaquist, R. Gruetter, Effect of hypoglycemia on brain glycogen metabolism *in vivo*, J. Neurosci. Res. 72 (1) (2003) 25–32.
[30] R.I. Herzog, et al., Effect of acute and recurrent hypoglycemia on changes in brain glycogen concentration, Endocrinology 149 (4) (2008) 1499–1504.
[31] R.G. Shulman, F. Hyder, D.L. Rothman, Cerebral energetics and the glycogen shunt: neurochemical basis of functional imaging, Proc. Natl. Acad. Sci. 98 (11) (2001) 6417–6422.
[32] G.A. Dienel, N.F. Cruz, Contributions of glycogen to astrocytic energetics during brain activation, Metab. Brain Dis. 30 (1) (2015) 281–298.
[33] L. Hertz, et al., Astrocytic glycogenolysis: mechanisms and functions, Metab. Brain Dis. 30 (1) (2014) 317–333.
[34] J. Duran, et al., Impairment in long-term memory Formation and learning-dependent synaptic Plasticity in mice lacking glycogen Synthase in the brain, J. Cereb. Blood Flow. Metab. 33 (4) (2013) 550–556.
[35] M.E. Gibbs, et al., Glycogen is a preferred glutamate precursor during learning in 1-day-old chick: biochemical and behavioral evidence, J. Neurosci. Res. 85 (15) (2007) 3326–3333.
[36] A. Suzuki, et al., Astrocyte-neuron lactate transport is required for long-term memory formation, Cell 144 (5) (2011) 810–823.
[37] G. Öz, et al., Human brain glycogen metabolism during and after hypoglycemia, Diabetes 58 (9) (2009) 1978–1985.
[38] P. Franken, et al., Glycogen content in the cerebral cortex increases with sleep loss in C57BL/6J mice, Neurosci. Lett. 402 (1–2) (2006) 176–179.
[39] J. Bergstrom, E. Hultman, Muscle glycogen synthesis after exercise : an enhancing factor localized to the muscle cells in man, Nature 210 (5033) (1966) 309–310.
[40] L.F. Obel, et al., Brain glycogen – new perspectives on its metabolic function and regulation at the subcellular level, Front. Neuroenergetics 4 (2012).
[41] A.M. Brown, S. Baltan Tekkök, B.R. Ransom, Energy transfer from astrocytes to axons: the role of CNS glycogen, Neurochem. Int. 45 (4) (2004) 529–536.
[42] L. Pellerin, P.J. Magistretti, Sweet sixteen for ANLS, J. Cereb. Blood Flow. Metab. 32 (7) (2012) 1152–1166.
[43] J.C. López Ramos, et al., Role of brain glycogen in the response to hypoxia and in susceptibility to epilepsy, Front. Cell. Neurosci. 9 (2015).
[44] J.B. Cavanagh, Corpora-amylacea and the family of polyglucosan diseases, Brain Res. Rev. 29 (2–3) (1999) 265–295.
[45] J. Duran, J.J. Guinovart, Brain glycogen in health and disease, Mol. Asp. Med. 46 (2015) 70–77.
[46] J.-F. Cloix, T. Hévor, Epilepsy, Regulation of brain energy Metabolism and neurotransmission, Curr. Med. Chem. 16 (7) (2009) 841–853.
[47] J.M.N. Duarte, Metabolic alterations associated to brain dysfunction in diabetes, Aging Dis. 6 (5) (2015) 304–321.
[48] J. Folbergrová, M. Ingvar, B.K. Siesjö, Metabolic changes in cerebral cortex, Hippocampus, and cerebellum during sustained bicuculline-induced seizures, J. Neurochem. 37 (5) (1981) 1228–1238.
[49] B.B. Johansson, K. Fredriksson, Cerebral energy metabolism during bicuculline-induced status epilepticus in spontaneously hypertensive rats, Acta Physiol. Scand. 123 (3) (1985) 299–302.
[50] K. Bernard-Hélary, et al., *In vivo* and *in vitro* glycogenic effects of methionine sulfoximine are different in two inbred strains of mice, Brain Res. 929 (2) (2002) 147–155.
[51] M.K. Dalsgaard, et al., High glycogen levels in the Hippocampus of patients with epilepsy, J. Cereb. Blood Flow. Metab. 27 (6) (2007) 1137–1141.
[52] K.G. Prasannan, K. Subrahmanyam, Enzymes of glycogen metabolism in cerebral cortex of normal and diabetic rats, J. Neurochem. 15 (10) (1968) 1239–1241.
[53] G. Sanchez-Chavez, et al., Effect of diabetes on glycogen metabolism in rat retina, Neurochem. Res. 33 (7) (2008) 1301–1308.
[54] H.M. Sickmann, et al., Obesity and type 2 diabetes in rats are associated with altered brain glycogen and amino-acid homeostasis, J. Cereb. Blood Flow. Metab. 30 (8) (2010) 1527–1537.
[55] P.E. Cryer, Human insulin and hypoglycemia unawareness, Diabetes Care 13 (5) (1990) 536–538.
[56] P.E. Cryer, Symptoms of hypoglycemia, thresholds for their occurrence, and hypoglycemia unawareness, Endocrinol. Metab. Clin. North Am. 28 (3) (1999) 495–500 v-vi.
[57] H. Lei, R. Gruetter, Effect of chronic hypoglycaemia on glucose concentration and glycogen content in rat brain: a localized ^{13}C NMR study, J. Neurochem. 99 (1) (2006) 260–268.
[58] H. Lei, et al., Direct validation of *in vivo* localized ^{13}C MRS measurements of brain glycogen, Magn. Reson. Med. 57 (2) (2007) 243–248.
[59] G. Öz, et al., Brain glycogen content and metabolism in subjects with type 1 diabetes and hypoglycemia unawareness, J. Cereb. Blood Flow. Metab. 32 (2) (2012) 256–263.
[60] W. Chen, et al., Nuclear magnetic resonance relaxation of glycogen H1 in solution, Biochemistry 32 (36) (1993) 9417–9422.
[61] L.H. Zang, A.M. Howseman, R.G. Shulman, Assignment of the ^{1}H chemical shifts of glycogen, Carbohydr. Res. 220 (1991) 1–9.
[62] L.H. Nilsson, E. Hultman, Liver glycogen in man—the effect of total starvation or a carbohydrate-poor diet followed by carbohydrate refeeding, Scand. J. Clin. Lab. Invest. 32 (4) (1973) 325–330.
[63] R. Ouwerkerk, R.I. Pettigrew, A.M. Gharib, Liver metabolite concentrations measured with 1H MR spectroscopy, Radiology 265 (2) (2012) 565–575.
[64] A.F. Soares, H. Lei, R. Gruetter, Characterization of hepatic fatty acids in mice with reduced liver fat by ultra-short echo time ^{1}H-MRS at 14.1 T *in vivo*, NMR Biomed. 28 (8) (2015) 1009–1020.
[65] W. Chen, et al., Proton NMR observation of glycogen in vivo, Magn. Reson Med. 31 (5) (1994) 576–579.
[66] I. Tkac, et al., *In vivo ^{1}H NMR spectroscopy of rat brain at 1 ms echo time*, Magn. Reson. Med. 41 (4) (1999) 649–656.
[67] Lei, H., et al., *Chapter 1.2-localized single-voxel magnetic resonance spectroscopy, water suppression, and novel Approaches for ultrashort echo-time measurements A2-Rothman, charlotte StaggDouglas*, in Magnetic Resonance Spectroscopy 2014, Academic Press: San Diego. p. 15–30.
[68] G. Liu, et al., Nuts and bolts of chemical exchange saturation transfer MRI, NMR Biomed. 26 (7) (2013) 810–828.
[69] P.C. van Zijl, et al., MRI detection of glycogen in vivo by using chemical exchange saturation transfer imaging (glycoCEST), Proc. Natl. Acad. Sci. U. S. A. 104 (11) (2007) 4359–4364.
[70] A.N. Dula, S.A. Smith, J.C. Gore, Application of chemical exchange saturation transfer (CEST) MRI for endogenous contrast at 7 Tesla, J. Neuroimaging 23 (4) (2013) 526–532.
[71] R. Gruetter, et al., *Validation of ^{13}C NMR measurements of liver glycogen*

in vivo, Magn. Reson. Med. 31 (6) (1994) 583–588.
[72] R. Taylor, et al., *Validation of ^{13}C nmr measurement of human skeletal muscle glycogen by direct biochemical assay of needle biopsy samples*, Magn. Reson. Med. 27 (1) (1992) 13–20.
[73] R.A. de Graaf, D.L. Rothman, K.L. Behar, State of the art direct ^{13}C and indirect ^{1}H-[^{13}C] NMR spectroscopy *in vivo*. A practical guide, NMR Biomed. 24 (8) (2011) 958–972.
[74] R. Gruetter, et al., Localized *in vivo* ^{13}C NMR spectroscopy of the brain, NMR Biomed. 16 (6–7) (2003) 313–338.
[75] G. Oz, et al., Revisiting glycogen content in the human brain, Neurochem. Res. 40 (12) (2015) 2473–2481.
[76] G. Oz, et al., *A localization method for the measurement of fast relaxing^{13}C NMR signals in humans at high magnetic fields*, Appl. Magn. Reson. 29 (1) (2005) 159–169.
[77] G. Oz, et al., Human brain glycogen content and metabolism: implications on its role in brain energy metabolism, Am. J. Physiol. Endocrinol. Metabol. 292 (3) (2007) E946–E951.
[78] R.B. van Heeswijk, et al., *A comparison of in vivo ^{13}C MR brain glycogen quantification at 9.4 and 14.1 T*, Magn. Reson. Med. 67 (6) (2012) 1523–1527.
[79] Magill, A.W. and R. Gruetter, Nested surface coils for multinuclear NMR, in *eMagRes*2007, John Wiley & Sons, Ltd.
[80] I.Y. Choi, et al., Noninvasive measurements of [1-^{13}C]glycogen concentrations and metabolism in rat brain *in vivo*, J. Neurochem. 73 (3) (1999) 1300–1308.
[81] F.D. Morgenthaler, et al., Non-invasive quantification of brain glycogen absolute concentration, J. Neurochem. 107 (5) (2008) 1414–1423.
[82] G. Adriany, R. Gruetter, A half-volume coil for efficient proton decoupling in humans at 4 tesla, J. Magn. Reson. 125 (1) (1997) 178–184.
[83] D.I. Hoult, C.N. Chen, V.J. Sank, Quadrature detection in the laboratory frame, Magn. Reson. Med. 1 (3) (1984) 339–353.
[84] D.W. Klomp, et al., *Sensitivity-enhanced ^{13}C MR spectroscopy of the human brain at 3 Tesla*, Magn. Reson. Med. 55 (2) (2006) 271–278.
[85] E.S. Roig, et al., A double-quadrature radiofrequency coil design for proton-decoupled carbon-13 magnetic resonance spectroscopy in humans at 7T, Magn. Reson. Med. 73 (2) (2015) 894–900.
[86] A.J. Shaka, J. Keeler, R. Freeman, Evaluation of a new broadband decoupling sequence: WALTZ-16, J. Magn. Reson. 53 (2) (1983) 313–340.
[87] A. Heerschap, et al., Broadband proton decoupled natural abundance ^{13}C NMR spectroscopy of humans at 1.5 T, NMR Biomed. 2 (3) (1989) 124–132.
[88] W.T. Dixon, Simple proton spectroscopic imaging, Radiology 153 (1) (1984) 189–194.
[89] N. Beckmann, S. Muller, *Natural-abundance ^{13}C spectroscopic imaging applied to humans*, J. Magn. Reson. 93 (1) (1991) 186–194.
[90] M.F. Alf, et al., High-resolution spatial mapping of changes in the neurochemical profile after focal ischemia in mice, NMR Biomed. 25 (2) (2012) 247–254.
[91] M. Garwood, T. Schleich, Improved fourier series windows for localization in *in vivo* NMR spectroscopy, J. Magn. Reson. 65 (1985) 510–515.
[92] M. Garwood, et al., A modified rotating frame experiment based on a fourier series window function. Application to in vivo spatially localized NMR spectroscopy, J. Magn. Reson. 65 (1985) 239–251.
[93] R.B. van Heeswijk, et al., Quantification of brain glycogen concentration and turnover through localized ^{13}C NMR of both the C1 and C6 resonances, NMR Biomed. 23 (3) (2010) 270–276.
[94] R.J. Ordidge, A. Connelly, J.A.B. Lohman, Image-selected *in Vivo* spectroscopy (ISIS). A new technique for spatially selective NMR spectroscopy, J. Magn. Reson. 66 (2) (1986) 283–294.
[95] D.L. Rothman, et al., Quantitation of hepatic glycogenolysis and gluconeogenesis in fasting humans with ^{13}C NMR, Science 254 (5031) (1991) 573–576.
[96] I.Y. Choi, I. Tkáč, R. Gruetter, Single-shot, three-dimensional "non-echo" localization method for in vivo NMR spectroscopy, Magn. Reson. Med. 44 (3) (2000) 387–394.
[97] D.L. Rothman, R.G. Shulman, G.I. Shulman, N.m.r. *studies of muscle glycogen synthesis in normal and non-insulin-dependent diabetic subjects*, Biochem. Soc. Trans. 19 (4) (1991) 992–994.
[98] A. Tannus, M. Garwood, Adiabatic pulses, NMR Biomed. 10 (8) (1997) 423–434.
[99] M.R. Bendall, D.T. Pegg, Uniform sample excitation with surface coils for *in vivo* spectroscopy by adiabatic rapid half passage, J. Magn. Reson. 67 (2) (1986) 376–381.
[100] K. Uğurbil, et al., Amplitude- and frequency/phase-modulated refocusing pulses that induce plane rotations even in the presence of inhomogeneous B1 fields, J. Magn. Reson 78 (3) (1988) 472–497.
[101] K. Uğurbil, M. Garwood, M. Robin Bendall, Amplitude- and frequency-modulated pulses to achieve 90° plane rotations with inhomogeneous B1 fields, J. Magn. Reson 72 (1) (1987) 177–185.
[102] M. Van Cauteren, et al., Excitation characteristics of adiabatic half-passage RF pulses used in surface coil MR spectroscopy. Application to 13C detection of glycogen in the rat liver, Phys. Med. Biol. 37 (5) (1992) 1055–1064.
[103] J. Rosenblatt, R.R. Wolfe, Calculation of substrate flux using stable isotopes, Am. J. Physiol. - Endocrinol. Metab. 254 (4) (1988) E526–E531.
[104] R. Gruetter, K. Ugurbil, E.R. Seaquist, Steady-state cerebral glucose concentrations and transport in the human brain, J. Neurochem. 70 (1) (1998) 397–408.
[105] I.Y. Choi, H. Lei, R. Gruetter, Effect of deep pentobarbital anesthesia on neurotransmitter metabolism *in vivo*: on the correlation of total glucose consumption with glutamatergic action, J. Cereb. Blood Flow. Metab. 22 (11) (2002) 1343–1351.
[106] J.M.N. Duarte, R. Gruetter, Characterization of cerebral glucose dynamics *in vivo* with a four-state conformational model of transport at the blood–-brain barrier, J. Neurochem. 121 (3) (2012) 396–406.
[107] R.G. Shulman, D.L. Rothman, 13C NMR of intermediary metabolism: implications for systemic physiology, Annu. Rev. Physiol. 63 (1) (2001) 15–48.
[108] M. DiNuzzo, Kinetic analysis of glycogen turnover: relevance to human brain 13C-NMR spectroscopy, J. Cereb. Blood Flow. Metab. 33 (10) (2013) 1540–1548.
[109] L.O. Sillerud, R.G. Shulman, Structure and metabolism of mammalian liver glycogen monitored by carbon-13 nuclear magnetic resonance, Biochemistry 22 (5) (1983) 1087–1094.
[110] L.H. Zang, et al., 13C NMR relaxation times of hepatic glycogen *in vitro* and *in vivo*, Biochemistry 29 (29) (1990) 6815–6820.
[111] K. Overloop, F. Vanstapel, P. Van Hecke, 13C-NMR relaxation in glycogen, Magn. Reson. Med. 36 (1) (1996) 45–51.